Time-Adaptive Probabilistic Forecasts of Electricity Spot Prices with Application to Risk Management.

Brenda López Cabrera*
Franziska Schulz*

* Humboldt-Universität zu Berlin, Germany

SFB 649 ECONOMIC RISK BERLIN

Time-Adaptive Probabilistic Forecasts of Electricity Spot Prices with Application to Risk Management. *

Brenda López Cabrera , Franziska Schulz [†]

September 18, 2016

Abstract

The increasing exposure to renewable energy has amplified the need for risk management in electricity markets. Electricity price risk poses a major challenge to market participants. We propose an approach to model and forecast electricity prices taking into account information on renewable energy production. While most literature focuses on point forecasting, our methodology forecasts the whole distribution of electricity prices and incorporates spike risk, which is of great value for risk management. It is based on functional principal component analysis and time-adaptive nonparametric density estimation techniques. The methodology is applied to electricity market data from Germany. We find that renewable infeed effects both, the location and the shape of spot price densities. A comparison with benchmark methods and an application to risk management are provided.

JEL classification: C1, Q41, Q47
Keywords: electricity prices; residual load; probabilistic forecasting; value at risk; expected shortfall; functional data analysis

1. Introduction

In recent years electricity markets have changed significantly. In Germany, the energy transition triggered by the regulators caused a rapid growth of renewable energy and has exposed the electricity market to new risk factors. The share of consumed electricity coming from renewable sources rose from 6.2% in 2000 to 32.6% in 2015 (BMWi 2016). This change in the structure of energy markets also affects the behavior of electricity spot prices: recently they have exhibited frequent downward spikes and negative prices have occurred regularly.

Low or even negative prices appear when low demand concurs with high infeed from renewable sources. Recent studies have shown that the level as well as the volatility of electricity prices are to a large extent determined by residual load, defined as the difference between total demand and renewable infeed (Nicolosi and Fürsch 2009; Hu 2009). The large volatility of renewables thus carries over to electricity prices. In order to cope with this increasing uncertainty, probabilistic forecasts and risk measures of electricity prices are crucial for market participants.

Several methods has been applied to electricity price forecasting over the last years. They range from machine learning techniques and statistical methods to structural models. An extensive review on recent methods is provided by Weron (2014). He points out that probabilistic forecasting is still rare in the electricity price forecasting literature. A recent overview on probabilistic forecasting in energy markets is given by Hong et al. (2016). Most papers that deal with probabilistic forecasts of electricity prices focus on prediction intervals (see e.g. Misiorek et al. (2006), Wan et al. (2014), Nowotarski and Weron (2015)). Literature on density forecasts is even more scarce. Exceptions are Serinaldi (2011), who use a generalized additive model for location, scale and shape in order to model and forecast the distribution of electricity prices. Panagiotelis and Smith (2008) use a combination of multivariate time series models and Markov chain Monte Carlo methods to compute predictive densities of spot prices. Jónsson et al. (2014) produce probabilistic forecasts using quantile regression combined with an exponential distribution to explain the distribution tails. In a recent work, Bello et al. (2015) conduct probabilistic forecasts in the medium-term using a fundamental market equilibrium model.

We propose to model the distribution of electricity spot prices conditional on residual load. This approach enables us to capture the effect of the interaction between demand and renewable infeed on electricity prices and to incorporate spikes that occur due to extremes in residual load.

Literature on modeling residual load is rare, one exception is Wagner (2014), who uses a stochastic model for wind and solar power to derive residual load. We propose to model daily residual load curves directly using Functional Principal Component Analysis (FPCA), a common tool in Functional Data Analysis (FDA) that reduces the dimensionality of the problem by decomposing curves into a low number of risk drivers. See Ramsay and Silverman (2005) for an introduction to FDA and Shang (2014) for a survey on FPCA. In our context, daily residual load curves are regarded as realizations of a functional time series. Dynamics over time of the curves are analyzed and forecasted using multivariate time series techniques. Similar methodologies have been applied to load forecasting by Shang (2013) and

López Cabrera and Schulz (2016). Others, like Antoch et al. (2008) or Goia et al. (2010) use functional linear models to predict electricity load curves. Nonparametric functional regression techniques are applied to load and price forecasting by Vilar et al. (2012).

Next, we use these daily curves to model the conditional density of daily spot price indices. This way, we can not only take into account information on the amount of residual load, but also on the distribution of residual load over the day. We suggest to model the relationship between residual load and prices using a flexible nonparametric approach with functional covariates. This technique is based on functional conditional kernel density estimation. The approach has the advantage that predictive densities can have any form, in particular they can be asymmetric, multimodal or fat-tailed. In order to accommodate potential time-varying behavior, we include an exponential decay factor. From the conditional density interval and point forecasts and risk measures like Value at Risk (VaR) or Expected Shortfall can be derived.

We apply the proposed methodology to prices of the Physical Electricity Index (Phelix) day base and Phelix day peak. Both indices are traded at the German electricity exchange EEX and serve as common underlyings for electricity derivatives. Phelix day base is the average of all 24 hourly spot prices, while Phelix day peak is the average of the spot prices during peak hours from 9am to 8pm.

The proposed methodology is evaluated based on 300 day-ahead out-of-sample forecasts. We compare the performance with regard to point, interval and density forecasting to several benchmark models, including a similar day approach and an autoregressive moving average model. The proposed model turns out to alomst always outperform the benchmark models.

Our article is structured as follows. Section 2 gives a brief introduction of the German electricity market and data. In Section 3 we describe the functional data approach to model and forecast residual load curves. Section 4 presents the functional conditional density estimator and introduces the time-adaptive approach. Section 5 discusses the modeling and estimation of residual load data and the density forecasting of electricity prices. In section 6 the forecasting performance is evaluated and compared to benchmark methods using several performance measures. An application to energy risk management is given in Section 7. Section 8 concludes the article. All computations in this article were carried out in R.

2. German electricity market and data

The German electricity market, which was liberalized in 1998, is Europe's largest, with annual power consumption of around 500 TWh and an annual production of around 600 TWh. In 2015, roughly one third of total production came from renewable sources (BMWi 2016). This poses new risk factors to market participants, as they have to cope with uncertain renewable infeed. Electricity is traded on the European Electricity Exchange (EEX), which contains a spot market (EPEX Spot) and a derivative market. EPEX Spot operates a day-ahead market, where market participants buy electricity for all 24 hours of the next day in a daily auction that takes place at 12pm. The EPEX Spot established two price indices, the Phelix base and

Phelix peak, which serve as reference prices for the European market. Market-based reference prices form an essential basis for market participants' decision making. Furthermore, the indices serve as underlying assets for Phelix futures, provided by the EEX. Hourly prices are set according to a merit order. This means that power plants are ordered according to their marginal costs and the price of electricity for a specific hour corresponds to the marginal costs of the last power plant that is needed to cover demand in that hour. The resulting merit order curve directly links electricity demand and prices. Conventionally, nuclear and lignite power plants serve base electricity demand, whereas the more expensive gas and oil power plants are only operated during hours of peak demand. Since renewable power plants have a feed-in guarantee and low marginal costs, they lower the entrance price and push conventional power plants down the merit order curve. Hence, increasing infeed from renewable energy results in lower electricity spot prices. This is also referred to as merit order effect. An overview on literature addressing the merit order effect is e.g. provided by Würzburg et al. (2013).

While the merit order effect has been subject of many researchers, the effect of renewable infeed on the volatility of electricity prices has been studied much less. A notable exception is Ketterer (2014), who applies a GARCH model to electricity prices in Germany in order to investigate the effect of renewable infeed on the mean and volatility of prices. She finds that while the electricity price is falling due to increased renewable infeed, the volatility of prices is increasing. A similar finding is reported by Woo et al. (2011), who investigate the Texas electricity market and point out that increasing share of renewable energy requires a higher degree of price risk management.

For a sustainable price risk management information of uncertainty and dispersion of future prices is crucial. In our analysis, we model and forecast the distribution of Phelix day base and Phelix day peak prices, taking into account information about electricity demand and renewable infeed. Distributional forecasts provide valuable information about uncertainty of prices and can be directly used to derive interval forecasts and risk measures.

	Total demand	Solar	Wind	RL	Phelix Base	Phelix Peak
Mean	56024.59	3974.07	5966.80	46083.73	34.66	38.72
Median	55871.00	241.88	4293.75	45793.25	34.36	38.18
SD	10276.44	5889.91	5353.44	10591.75	9.90	13.13
Min	29550.00	0.00	28.75	8958.00	−4.13	−18.99
Max	79120.00	25811.75	30582.50	78069.50	62.89	80.50

Table 1: Summary statistics. Total demand, solar, wind and residual load (RL) in MW. Phelix base and Phelix peak in EUR/MWh.

For the empirical work of this article, we use daily data on Phelix day base and Phelix day peak prices as well as hourly data on electricity consumption, wind infeed and solar infeed. The price data is obtained from Bloomberg. Electricity consumption data is obtained from the European Network of Transmission System Operators for Electricity (ENTSO-E). Data on wind and solar infeed is obtained from

the four German transmission system operators (50Hertz, Amprion, TennetTSO, TransnetBW). The analysis is based on data from 2013-01-01 to 2015-10-31. Summary statistics are given in Table 1. The time series of Phelix day base and Phelix day peak prices are displayed in Figure 1. It can be seen that the Phelix day peak has a larger volatility and more pronounced spikes than the Phelix day base. This is also visible from the summary statistics and not surprising, since the Phelix day peak corresponds to hours with high and variable demand. Both price series exhibit positive skewness and an excess kurtosis of about 1, implying a heavy-tailed unconditional distribution that is skewed to the right.
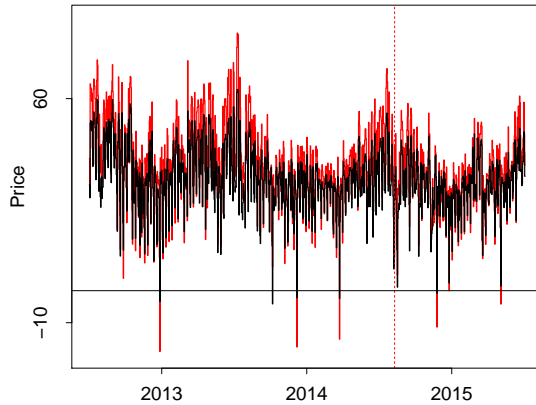

Figure 1: Phelix day base (black) and Phelix day peak (red) index from 2013-01-01 to 2015-10-31. The red dottet line marks the end of the in-sample period.
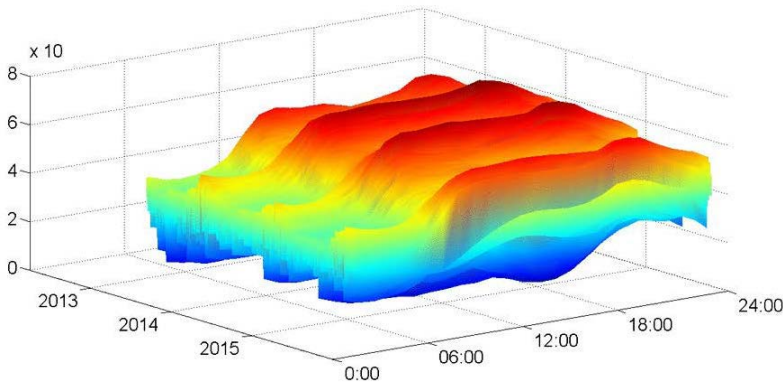

Figure 2: Residual Load in GW from 2013-01-01 to 2015-10-31

As pointed out above, prices of electricity do not only depend on total consumption, but rather on the amount of electricity that has to be produced from conventional energy sources. We refer to this as residual load which we define as:

$$R_t = L_t - W_t - S_t, \tag{1}$$

5

where L_t is total demand, W_t is wind infeed and S_t is solar infeed at time t. That is, residual load corresponds to total consumption minus electricity infeed from renewable sources. Since biomass and hydro power are still negligible in the German electricity market, we do not consider them in this study.

Figure 2 displays the residual load data. Typical load profiles on a day with high and low renewable infeed respectively are shown in Figure 3. It is clearly visible that residual load contains annual, weekly and intraday seasonal cycles. They closely follow the seasonalities of consumption which is lower during winter than during summer and lower during weekends than during the week.

Typically, the intraday load profile shows a peak around noon, followed by valley in the afternoon and another peak in the evening. The valley during the afternoon becomes more pronounced the more solar infeed is present.
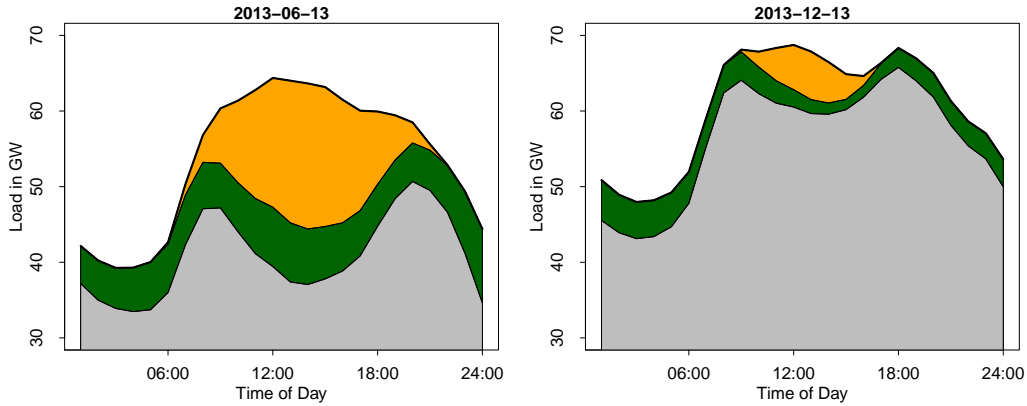

Figure 3: Total consumption (thick black line), solar infeed (orange), wind infeed (green) and residual load (gray) on a day with high renewable infeed (left) and low renewable infeed (right).

Since the seasonal patterns of load curves are quite predictable, we model them deterministically. We express the observed residual load $\tilde{R}_t$ as

$$\tilde{R}_t = \Lambda_t + R_t, \qquad t = 1, \ldots, T, \tag{2}$$

where Λ_t is a deterministic seasonal component and R_t is a stochastic component. We estimate the deterministic seasonal component separately for every quarter-hour of a day. It is specified as

$$\Lambda_{s,k} = a_s + b_s \cdot k + c_{1,s} \sin\left(\frac{2\pi k}{365}\right) + c_{2,s} \cos\left(\frac{2\pi k}{365}\right) + \sum_{i=1}^{7} d_{i,s} \cdot D_{i,k}, \tag{3}$$

where $s = 1, \ldots, S$ denotes time within the day in hours and $k = 1, \ldots, n$ the day, such that $S = 24$ and $S \cdot n = T$. The parameters $a_s, b_s, c_{1,s}, c_{2,s}$ and $d_{i,s}$ are estimated by ordinary least square regression. $D_{i,k}$ is a set of dummy variables consisting of six dummies for the weekdays and one dummy for public holidays. They capture weekly seasonal behavior, while the sine and cosine functions capture

yearly seasonalities. This approach is very close to the so called similar-day approach which is a commonly used approach in industry to model and forecast electricity load.

3. Methodology

3.1 Modeling and forecasting residual load

We divide the univariate time series of residual load into segments and treat them as a time series of curves, where each curve represents one day. Since daily load curves show a similar pattern, this is a natural approach. Each of the daily segments of residual load contains 24 hourly observations. We denote these segments as $R_{s,k}$, where $s = 1, \ldots, 24$ denotes the time within the day and k denotes the day. They are regarded as realizations $R_k(s)$ of a functional time series $\{R_k, k \in \mathbb{Z}\}$ defined on a compact set $\mathcal{S}$, where $\mathcal{S}$ corresponds to one day. For an overview on functional time series we refer to Horváth and Kokoszka (2012). Under stationarity $R_k(s)$ have a common mean function $\mathrm{E}\{R(s)\} = \mu(s)$ and a common covariance function $C(s,t) = \mathrm{Cov}\{R(s), R(t)\}$ with $s, t \in \mathcal{S}$. Note that functional observations are intrinsically infinite dimensional. We model the time series of intra-daily residual load curves using functional principal component analysis (FPCA). FPCA is a tool to reduce the dimensionality of the problem that exploits the common structure of the residual load curves. It decomposes the functional process into the sum of the common mean function $\mu(s)$ and a linear combination of orthogonal principal component functions. The principal component functions are the eigenfunctions ϕ_i, $i = 1, 2, \ldots$, of the Kernel operator $\mathrm{K} : \phi \mapsto \mathrm{K}\phi$ defined by $(\mathrm{K}\phi)(s) = \int_{\mathcal{S}} C(s,t)\phi(t)dt$. The Karhuhen-Lo'{e}ve expansion provides a representation of the intra-daily residual load curves as:

$$R_k(s) = \mu(s) + \sum_{i=1}^{\infty} \alpha_{ik}\phi_i(s), \tag{4}$$

where $\alpha_i, i = 1, 2, \ldots$ are the principal component scores defined as $\langle R(s), \phi_i \rangle$, where $\langle \cdot, \cdot \rangle$ denotes the inner product. That is, the principal component scores are the projection of the residual load curves in the direction of the corresponding principal components. They satisfy $\mathrm{E}(\alpha_i) = 0$ and $\mathrm{Var}(\alpha_i) = \lambda_i$, where λ_i is the non-increasing and non-negative sequence of eigenvalues corresponding to the eigenfunctions ϕ_i of the operator K. By taking only the first m principal component functions, the truncated Karhuhen-Lo'{e}ve expansion approximates the functions $R_k(t)$:

$$R_k(s) \approx \mu(s) + \sum_{i=1}^{m} \alpha_{ik}\phi_i(s). \tag{5}$$

In practice, the mean, the principal components and the principal component scores have to be estimated from a sample of the functional process. We estimate the mean of the functions by

$$\widehat{\mu}(s) = \frac{1}{n}\sum_{k=1}^{n} R_k(s), \tag{6}$$

where n is the sample size. The kernel operator is estimated by

$$(\widehat{\mathbb{K}}\phi)(s) = \int_{\mathcal{S}} \widehat{C}(s,t)\phi(t)dt, \tag{7}$$

where

$$\widehat{C}(s,t) = \frac{1}{n}\sum_{k=1}^{n}\{R_k(s) - \widehat{\mu}(s)\}\{R_k(t) - \widehat{\mu}(t)\}. \tag{8}$$

From (7) we estimate eigenfunctions and eigenvalues and denote them by $\widehat{\phi}_i$ and $\widehat{\alpha}_{ik}, i = 1, \ldots, m$. Hörmann and Kokoszka (2010) show that these estimates are $\sqrt{n}$-consistent for a large group of stationary functional time series, including in particular linear functional processes. To choose the number of principal component functions m in Equation (5) there exist various rules. Here, the number is chosen such that at least an a priori fixed amount of variation in the data is explained by the principal component functions.

It is noted that only the principal component scores are varying over time, whereas the mean and principal component functions are time invariant. Hence, the dynamics over time of the residual load curves are fully captured by the dynamics of the principal component scores. The estimated principal component scores $\widehat{\alpha}_{ik}$ form a m-variate time-series of length n. Hence, the dimension of the problem has been reduced from infinite to m. We model the dynamics of the principal component scores using a vector autoregressive (VAR) process of order p. It is given by

$$\widehat{\boldsymbol{\alpha}}_k = \sum_{i=1}^{p} \boldsymbol{\Phi}_i \widehat{\boldsymbol{\alpha}}_{k-i} + \boldsymbol{\eta}_k \tag{9}$$

where $\widehat{\boldsymbol{\alpha}}_k$ is the vector of estimated principal component scores, $\boldsymbol{\Phi}_i$ is a coefficient matrix and $\boldsymbol{\eta}_k$ is a white noise process (Lütkepohl 2005). The lag order p of the VAR process is determined by an Akaike information criterion. The VAR(p) model is then used to produce forecasts of the principal component scores $\widehat{\alpha}_{i,n+h}$, where h denotes the forecast horizon. Plugging these forecasts into (5) yields forecasts of the whole residual load curve:

$$\widehat{R}_{n+h}(s) = \widehat{\mu}(s) + \sum_{i=1}^{m} \widehat{\alpha}_{i,n+h}\widehat{\phi}_i(s), \tag{10}$$

where $\widehat{R}_{n+h}(t)$ is the h-step ahead forecast of the residual load curve.

3.2 Functional kernel density estimation of electricity prices conditional on residual load

As described above, electricity demand and prices are inherently connected through the merit order curve. We model the relation between demand and prices using methods for functional data. This has the advantage that we can take the information of the whole residual load curve into account to model the distribution of the daily prices. We chose a functional conditional kernel density (fCKD) estimator to estimate the density of electricity prices conditional on the residual load curves. The estimator requires neither assumption on the resulting density of prices nor on the functional form of the relationship between prices and residual load. This flexibility is desirable in this context, since prices are generally asymmetric and heavy-tailed. Furthermore, the functional form of the relationship between prices and residual load is unknown and not straightforward to derive.

The fCKD estimator (Ferraty and Vieu 2006) is given by :

$$\widehat{f}(y|R) = \frac{\frac{1}{g}\sum_{k=1}^{n} \mathrm{K}\left[h^{-1}d\{R(s), R_k(s)\}\right] \mathrm{K}_0\{g^{-1}(y - Y_k)\}}{\sum_{k=1}^{n} \mathrm{K}\left[h^{-1}d\{R(s), R_k(s)\}\right]}, \tag{11}$$

where K and K_0 are kernels, h and g are positive bandwidth parameters and $d(\cdot,\cdot)$ is a semi-metric that measures the proximity of curves. It is a functional extension of the well known Nadaraya-Watson estimator (Nadaraya 1964; Watson 1964), where the main change comes from the introduction of the semi-metric d. We choose a semi-metric that is based on principal component analysis. It is defined as

$$d_q^{PCA}(R_k, R) = \sqrt{\sum_{m=1}^{q} \left[\int \{R_k(s) - R(s)\}v_m(s)ds\right]^2}, \tag{12}$$

where $v_1, \ldots, v_q$ are the first q eigenvectors of the covariance matrix of the curves R_k, with q being a tuning parameter that has to be fixed a priori. The idea of the PCA-based semi-metric is to compute proximities between curves in a reduced dimensional space, where q determines the resolution at which curves are compared. For more details and different choices of the semi-metric we refer to Ferraty and Vieu (2006).

The two bandwidth parameters h and g are chosen based on cross-validation. The cross-validation is done as follows. We compute day-ahead density forecasts for the cross-validation sample and choose the bandwidth such that the forecasting accuracy in the cross-validation sample is maximized. As a measure of forecasting accuracy we choose the logarithmic score which evaluates location as well as concentration of the density forecasts and is a local proper scoring rule (Gneiting and Katzfuss 2014).

Looking at scatterplots of electricity prices and average daily residual load for different time periods (see Section 4) indicates that the relationship between prices and residual demand is varying over time. This happens due to factors that impact the market environment and that we do not capture in our model. A way to address

this time-varying behavior is to give more weight to recent observations and to weight observations less that are more far away in time. We implement a time-adaptive algorithm that is based on an exponential decay factor. For this, we adjust the time-adaptive conditional kernel density approach proposed by Jeon and Taylor (2012) to the functional estimator. The time-adaptive functional kernel density estimator (TA-fCKDE) is given by:

$$\widehat{f}(y|R) = \frac{\frac{1}{g}\sum_{k=1}^{n} \lambda^{n-k} \operatorname{K}\left[h^{-1}d\{R(s), R_k(s)\}\right] \operatorname{K}_0\{g^{-1}(y - Y_k)\}}{\sum_{k=1}^{n} \lambda^{n-k} \operatorname{K}\left[h^{-1}d\{R(s), R_i(s)\}\right]}, \qquad (13)$$

where $\lambda \in (0,1]$ is an exponential time decay factor. The smaller λ, the faster the factor decays and the more weight is given to recent values. We determine λ together with the bandwidth parameters in the cross-validation.

The fCKD estimator and TA-fCKD estimator yield estimates of the electricity spot price density conditional on a given residual load curve. If we use the fCKD estimator for forecasting, the future residual load curve is of course unknown. The purpose of the FPCA described in the previous section is to produce high quality forecasts of the residual load curve that can be used to obtain a forecast of the electricity price density.

4. Modeling and forecasting dynamics of residual load and spot price densities

Since the relationship between prices and residual load curves is too complex to display visually, in order to illustrate the relationship between both we show a scatterplot of prices and average daily residual load in Figure 4. A clear positive relationship is visible, with slightly increasing variance for higher residual load. The right panel of the plot indicates that the relationship is not invariant over time.
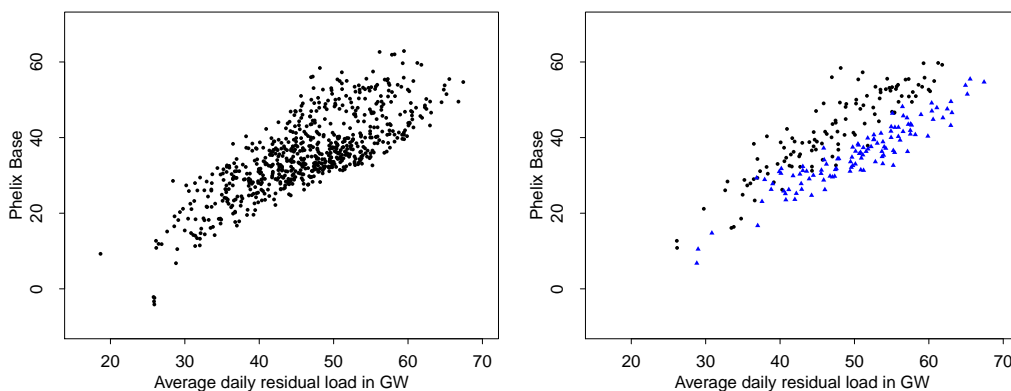

Figure 4: Phelix day base prices vs. average daily residual load for the whole in-sample period (left) and for the first four month (black dots) and the last four month (blue triangles) of the in-sample period (right).

In the first step we model residual load curves for the in-sample period from 2013-01-01 to 2014-12-31 as described in Section 3.1. We choose the number of principal

components such that at least 95% of the variation in the data is explained. It turns out that three principal components are sufficient. The first three principal components together with their principal component scores are displayed in Figure 5. The first principal component explains already 80% of the variance. Variations in the first principal components correspond mainly to shifts in the level of the load curve. Principal components two and three explain 10% and 6% respectively and are responsible for variations in the curvature of the load curve.

The dynamics of the principal component scores are modeled using model (9). We determined the lag order p of the VAR model based on the Akaike information criterion (AIC) and considered lags up to order 14. We find that a VAR(1) model has the lowest AIC. Estimation results of the coefficient matrix Φ_1 are reported in table 2. They show that although the principal components are instantaneously uncorrelated by construction, they do exhibit dependencies over time.

	$\alpha_{1,t-1}$	$\alpha_{1,t-2}$	$\alpha_{1,t-3}$
$\alpha_{1,t}$	0.62	−0.53	0.86
	(0.00)	(0.00)	(0.00)
$\alpha_{2,t}$	0.11	0.01	0.51
	(0.00)	(0.87)	(0.00)
$\alpha_{3,t}$	−0.01	0.14	0.25
	(0.51)	(0.00)	(0.00)

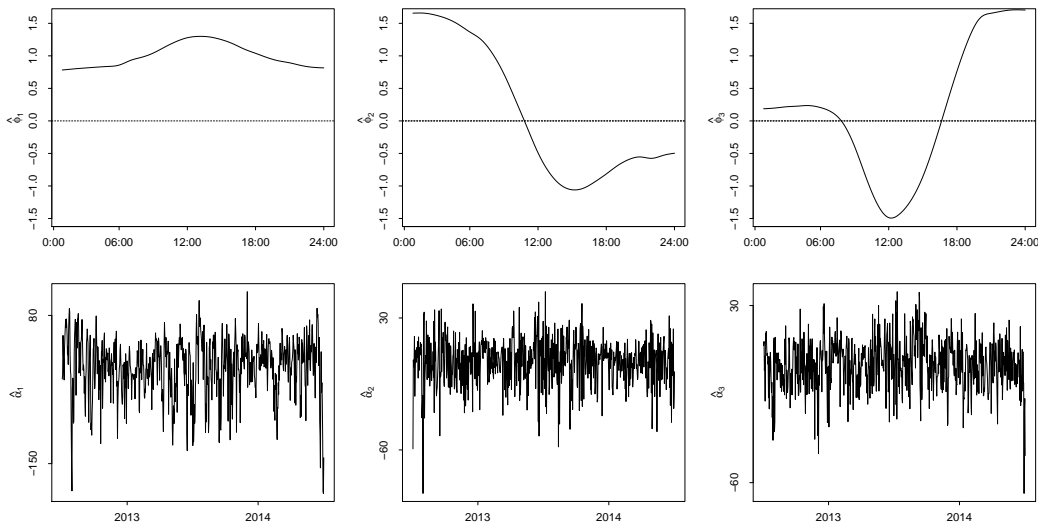Table 2: Estimates of the coefficients of the VAR(1) model. P-values in parentheses.

Figure 5: First three principal component scores and the corresponding principal component scores for the in-sample period (2013-01-01 to 2014-12-31). Explained variance: 80%, 10% and 6%

Day-ahead forecasts of the residual load curves are computed according to (10). We achieve a mean squared percentage error of 1.75% based on 300 day-ahead out-of-sample forecasts.

In the second step, forecasted residual load curves are used to produce forecasts of the conditional electricity price density as described in Section 3.2.

Figure 6 shows exemplary forecasted densities of the Phelix day base price together with the corresponding residual load for a day with high residual load, low residual load and medium residual load. It can be seen that the location as well as the shape of the price density varies with residual load. Especially on the day with low residual load, it is highly asymmetric and bimodal. Interestingly, the realized price almost coincides with the lower mode.
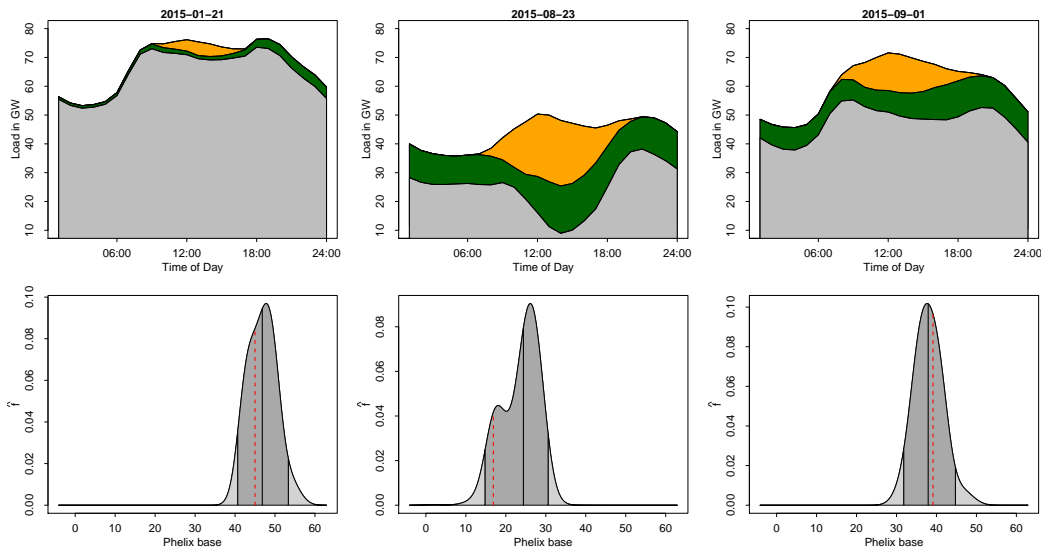
Figure 6: Residual load (upper panel) and forecasted spot price density (lower panel) together with 0.05 and 0.95 Quantile (gray shades), median (black solid line) and observed price (red dashed line).

5.   Forecast evaluation

We compare the forecast performance of the functional conditional kernel density estimator (fCKDE) and the time-adaptive functional conditional kernel density estimator (TA-fCKDE) to the results of several benchmark models. The first two years of data are used for in-sample fitting. For the remaining data, we compute $H = 300$ day-ahead out-of-sample forecasts using a rolling window approach. For the cross-validation of the bandwidth parameters and the exponential decay factor λ we keep the last third of the in-sample period as a cross-validation sample.

The forecasts are computed under two scenarios for the residual load: (1) we assume that we have a perfect forecast, that is we use measured residual load as input for our price forecast, (2) we use forecasted residual load from our model proposed in Section 3.1 as input for our price forecasts. In this way we can on the one hand compare the performance of the price forecasting models fairly on the basis of a perfect forecast. On the other hand, we obtain an idea of how much of the uncertainty in price forecasting comes from the uncertainty in load forecasting.

5.1 Benchmark Models

We estimate the following benchmark models and compare their performance for day-ahead forecasting to the performance of the fCKDE and the TA-fCKDE.

I   Naive similar day approach
II   ARMAX
III Kernel density estimator (KDE)
IV Conditional kernel density estimator (CKDE)

The first benchmark model (I) is a simple or naive model that is based on the idea that a good prediction of today's electricity price, is the price on the same weekday one week ago. It is often called similar day approach and popular due to its simplicity. The model is given by

$$y_k = y_{k-7} + \varepsilon_k, \tag{14}$$

where ε_k is a white noise process.

As a further benchmark model (II) we choose the autoregressive moving average model (ARMA). ARMA models and variations of it are very often used in literature, see e.g. Cuaresma et al. (2004), Weron and Misiorek (2008), Kristiansen (2012) and serve as common benchmark models. We include weekday dummy variables in order to account for weekly seasonalities. The ARMA(p,q) model with exogenous variables (ARMAX) is given by:

$$y_k = c + \sum_{i=1}^{p} \phi_i y_{k-i} + \sum_{j=1}^{q} \theta_j \varepsilon_{k-j} + \beta x_k + \varepsilon_k, \tag{15}$$

where c is a constant, ϕ, θ and β are parameters that have to be estimated, x_k are exogenous variables and ε_k is a white noise process. The lag orders p and q are chosen according to the Akaike information criterion.

Models I and II can be used to produce point forecasts of electricity spot prices. They do not yield information about the future price distribution.

Model III is a simple unconditional kernel density estimator (KDE) given by:

$$\widehat{f}(y) = \frac{1}{ng} \sum_{k=1}^{n} \mathrm{K}_0\{g^{-1}(y - Y_k)\}, \tag{16}$$

where K_0 is a kernel function and g is a bandwidth parameter. It has the advantage that only information about past electricity prices is needed. Therefore, it does not rely on forecasted values of residual load.

Furthermore, we chose the Nadaraya-Watson conditional kernel density estimator (CKDE) as a benchmark (IV), where the conditional variable is the average daily residual load. It is given by:

$$\widehat{f}(y|\bar{R}) = \frac{\frac{1}{g}\sum_{k=1}^{n} \mathrm{K}\{h^{-1}(\bar{R} - \bar{R}_k)\}\, \mathrm{K}_0\{g^{-1}(y - Y_k)\}}{\sum_{k=1}^{n} \mathrm{K}\{h^{-1}(\bar{R} - \bar{R}_k)\}}, \tag{17}$$

where $\bar{R}_k$ denotes average daily residual load on day k, K and K_0 are kernels, h and g are positive bandwidth parameters. This estimator takes into account the information about the amount of electricity that has to be produced from conventional power plants, but it does not consider its distribution over the day.

5.2 Point Forecasting

The main focus of our analysis is density forecasting. However, we also look at the performance of point forecasts for two reasons. First, point forecasts provide useful information about the location of the predicted density and are of great importance for users. Second, most established methods for electricity price forecasting only yield point forecasts. This way, we are able to compare our results to other well established methods, as the similar day approach and the ARMA model. We compute mean and median of the predicted densities and evaluate them using the root mean squared error (RMSE) and the mean absolute percentage error (MAPE), respectively. Thus, we take the respective loss function of the mean and the median into account when evaluating the forecast (Gneiting 2011). The forecasts of the similar day approach and the ARMA model are evaluated based on the RMSE only, as they do not provide forecasts of the median. RMSE and MAPE are defined as

$$\mathrm{RMSE} = \sqrt{\frac{1}{H}\sum_{h=1}^{H}(y_{n+h} - \widehat{y}_{n+h})^2}, \tag{18}$$

$$\mathrm{MAPE} = \frac{1}{H}\sum_{h=1}^{H} |\frac{y_{n+h} - \widehat{y}_{n+h}}{y_{n+h}}|, \tag{19}$$

where H denotes the total number of forecasts, y_{n+h} is the observed price at day $n + h$ and $\widehat{y}_{n+h}$ denotes the day-ahead point forecast of day $n + h$.

The results are shown in Table 3. The TA-fCKDE performs best in forecasting the mean as well as the median. Surprisingly, the similar day approach performs relatively good as well, given its simplicity. Both the similar day approach and the ARMAX model outperform the unconditional kernel density estimator (KDE) in point forecasting, though they do not provide information about the density. Naturally, forecasts under scenario (1) are better than forecasts under scenario (2). The ranking of the models does however not change.

5.3 Density Forecasting

We evaluate the density forecasts using probability integral transforms (PIT) of the predicted densities (Diebold et al. 1998) as well as logarithmic scores (LS) (Gneiting and Katzfuss 2014). The PIT is defined as:

14

| | Scenario (1) | | | | Scenario (2) | | | |
| | MAE | | RMSE | | MAE | | RMSE | |
	Base	Peak	Base	Peak	Base	Peak	Base	Peak
SD	-	-	9.16	10.64	-	-	9.16	10.64
ARMA	-	-	7.23	9.73	-	-	7.23	9.73
KDE	15.15	18.02	8.84	11.50	15.15	18.02	8.84	11.50
CKDE	7.03	8.06	4.64	5.83	7.03	6.77	5.91	7.37
fCKDE	6.64	7.70	4.77	5.89	6.64	6.72	6.06	7.52
TAfCKDE	5.94	7.21	3.61	4.70	5.78	6.48	4.88	6.19

Table 3: Mean absolute error (MAE) and root mean squared error (RMSE) based on $H = 300$ day-ahead forecasts.

$$\text{PIT}_h = \int_{-\infty}^{y_{n+h}} \widehat{f}_{n+h}(u)du, \qquad (20)$$

where $h = 1, \ldots, H$ denotes the day-ahead forecasts and $\widehat{f}_{n+h}(\cdot)$ is the predicted density of the price at day $n + h$. That is, the PIT is the cumulative density function of the predicted density evaluated at y_{n+h}. Note, that if the predicted density equals the true data generating process, then $\text{PIT}_h \sim U(0, 1)$. In Figures 7 and 8 we plot histograms of the PIT. High bars indicate that the corresponding part of the distribution is underestimated and vice versa. Under scenario (1) the KDE overestimates the right tail, while the CKDE overestimates both tails. The PIT from the fCKDE and the TA-fCKDE look more uniform. Under scenario (2) the TA-fCKDE underestimates the tail-risk for peak load, but seems to capture the distribution of base load quite well.
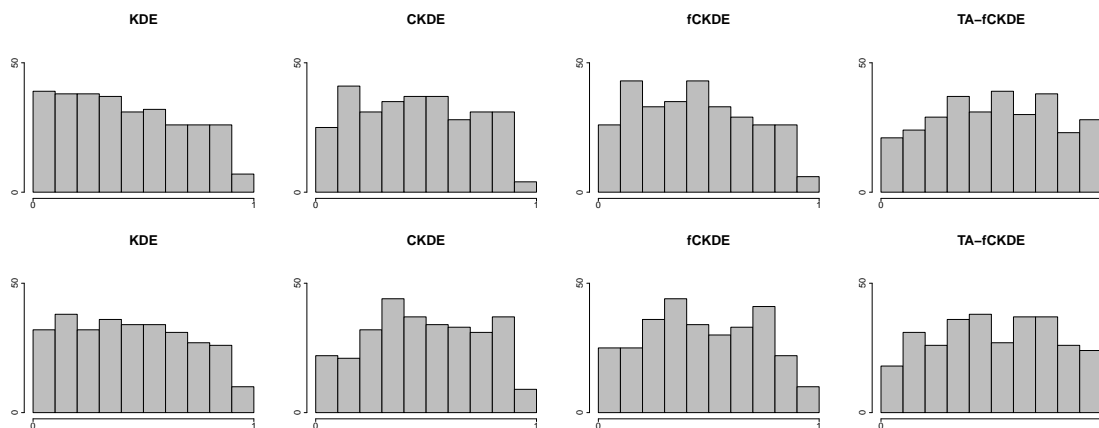

Figure 7: Probability integral transform for peak load (upper panel) and base load (lower panel) based on $H = 300$ day-ahead forecasts under scenario (1).

Though, as pointed out by (Hamill 2001), uniformity of the PIT does not guarantee unbiasedness of the forecasts. Hence, it is a necessary condition for a good
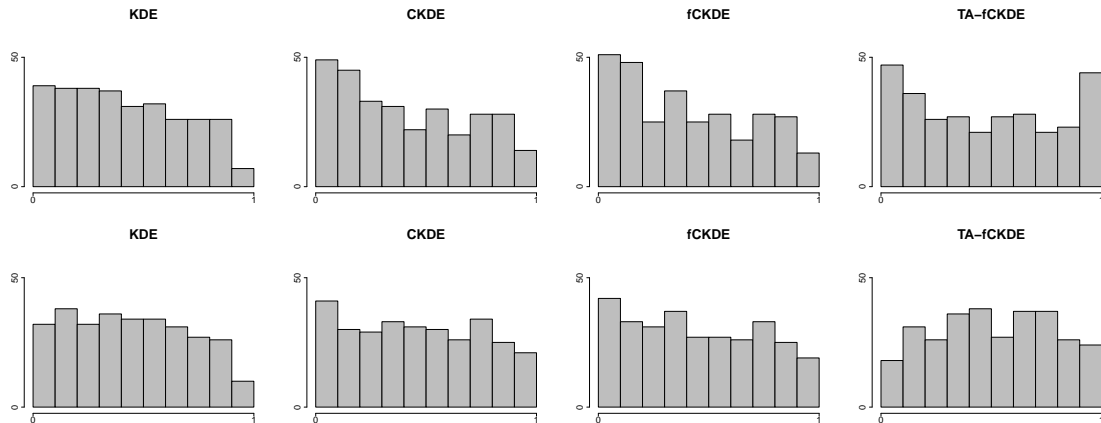
Figure 8: Probability integral transform for peak load (upper panel) and base load (lower panel) based on $H = 300$ day-ahead forecasts under scenario (2).

forecast, but not a sufficient one. Therefore, we additionally compute the LS, which is a local proper scoring rule. It is defined as

$$\mathrm{LS}_h(\widehat{f}_{n+h}, y_{n+h}) = -\log\{\widehat{f}_{n+h}(y_{n+h})\}, \tag{21}$$

where $\widehat{f}_{n+h}(\cdot)$ is the predicted density of the price at day $n + h$ and y_{n+h} is the observed price. The LS evaluates the quality of a probabilistic forecasts based on the paradigm of maximizing sharpness subject to calibration. In other words, it takes into account both, the concentration of the predicted distribution (sharpness) and its location relative to the observed values (calibration). The average LS over the out-of-sample period are reported in table 4. Again, the TA-fCKDE outperforms the other methods.

	Scenario (1)		Scenario (2)	
	Base	Peak	Base	Peak
KDE	3.59	3.88	3.59	3.88
CKDE	2.95	3.16	3.25	3.47
fCKDE	2.94	3.16	3.23	3.45
TA-fCKDE	2.70	2.94	3.07	3.34

Table 4: Mean logarithmic score (LS) based on $H = 300$ day-ahead forecasts.

5.4   Quantile and Interval Forecasting

Special interest often lies in certain quantiles of the distribution and the intervals spanned by them. In section 6 we show how they can be used for risk management.

We evaluate the accuracy of conditional quantile forecasts using the pinball loss function given by:

$$L(\widehat{q}_{\tau,n+h}, y_{n+h}) = |\tau - \mathrm{I}_{(y_{n+h} \leq \widehat{q}_{\tau,n+h})}| |y_{n+h} - \widehat{q}_{\tau,n+h}|, \tag{22}$$

where $\widehat{q}_{\tau,n+h}$ denotes the day-ahead quantile forecast with level of asymmetry τ on day $n+h$ and y_{n+h} is the observed price on that day. The pinball loss function can be interpreted as a weighted absolute error, where the weight reflects the asymmetry of the quantiles. It is a popular tool to evaluate quantile forecasts that has for example been suggested by Hong et al. (2016) and Steinwart et al. (2011).

Table 6 shows the average loss function over all $H = 300$ day-ahead forecasts. The smaller the value, the better. For reasons of compactness, we only show the results under scenario (1), as the results for scenario (2) do not differ in their conclusion. We find that the TA-fCKDE performs best for most of the considered quantile levels for both, base and peak load prices. Only for the 0.01 quantile it is outperformed by both the fCKDE and the CKDE.

$\tau =$	0.01	0.05	0.25	0.5	0.75	0.95	0.99
KDE	0.35	1.09	2.77	3.32	2.71	0.96	0.26
CKDE	0.10	0.44	1.33	1.80	1.60	0.65	0.17
fCKDE	0.10	0.42	1.33	1.75	1.56	0.63	0.17
TA-fCKDE	0.13	0.40	1.12	1.37	1.09	0.39	0.11

Table 5: Mean pinball loss based on $H = 300$ day-ahead quantile forecasts (base).

$\tau =$	0.01	0.05	0.25	0.5	0.75	0.95	0.99
KDE	0.42	1.28	3.55	4.35	3.63	1.30	0.36
CKDE	0.12	0.52	1.57	2.16	2.04	0.84	0.22
fCKDE	0.12	0.48	1.62	2.16	1.98	0.81	0.22
TA-fCKDE	0.21	0.54	1.40	1.73	1.41	0.50	0.14

Table 6: Mean pinball loss based on $H = 300$ day-ahead quantile forecasts (peak).

6. Application to Risk Management

Deregulated electricity markets provide opportunities for market participants to trade electricity and its derivatives. While this can be beneficial, the specific characteristics of electricity spot prices also pose major challenges at market participants. In order to cope with these challenges, effective risk management is advantageous. A first step in risk management is the measurement of risk. This quantification of uncertainty provides relevant information for the decision-making of market participants and forms the basis for trading strategies that meet their risk attitude. From a firm's perspective, as pointed out by Chan and Gray (2006), over-capitalization due to overestimation of risk implies idle capital which compromises the firms's profitability. On the other hand, under-capitalization may cause financial distress in

case the firm is unable to meet the obligations of its trading contracts. Therefore, risk measurement is a central part in establishing optimal trading limits. Our probabilistic forecasts yield a complete picture of future electricity prices and can directly be used to measure uncertainty. Given the spike risk of electricity prices associated with tail events, knowledge about the tail dynamics rather than the variations around the mean is crucial for a sustainable risk management. We compute two different risk measures, Value at Risk (VaR) and Expected Shortfall (ES), based on the forecasts generated by the fCKDE and the TA-fCKDE using numerical integration techniques.

VaR is defined as:

$$\text{VaR}(\tau) = F_y^{-1}(\tau), \tag{23}$$

where $\tau \in (0, 1)$ corresponds to the probability that the spot price will fall below the amount given by the VaR. That is, $\text{VaR}(\tau)$ is exactly the $\tau \cdot 100\%$ quantile of the price distribution. VaR is a measure of price risk and a standard tool in finance (Duffie and Pan 1997; Holton 2003). However, it is not a coherent risk measure (see e.g. Artzner et al. (1999)). For a discussion of VaR in energy markets see e.g. Eydeland and Wolyniec (2003). A popular tool to compute VaR are GARCH models, which were shown to perform well for energy markets, if they have fat-tailed and possibly skewed distributions (Aloui 2008; Füss et al. 2010; Giot and Laurent 2003). Bunn et al. (2016) compute VaR levels for electricity spot prices using quantile regression with fundamental factors and volatility as explanatory factor in order to capture the specific behavior of electricity prices. Here, we use a different methodology that takes into account the effect of the interaction between demand and renewable infeed on electricity prices and incorporates the risk of extremes in spot prices. We show a plot of the 1% VaR for our out-of-sample forecasting period based on the fCKDE and the TA-fCKDE in Figure 9. While in the beginning of the period they provide comparable results, for the second part of 2015 the TA-fCKDE estimates a lower tail risk than the fCKDE. Furthermore, it can be seen that price spikes are captured quite well.

Next, we compute the Expected Shortfall, that is, the expected value of a random variable below a given threshold. It is a more accurate risk measure compared to the VaR, since it takes diversification and risk aggregation effects properly into account and thus is a coherent risk measure (Acerbi and Tasche 2002; Delbaen 2002). ES is defined as

$$\text{ES}(\tau) = \frac{1}{\tau} \int_0^\tau \text{VaR}(\theta)d\theta, \quad \tau \in (0, 1). \tag{24}$$

The right panel of Figure 9 shows estimates of the 1% Expected Shortfall. By construction, ES is lower than VaR. Though, it shows a similar pattern to the VaR. While the TA-fCKDE again estimates a lower tail risk, the difference is less distinctive.

VaR ignores losses below the VaR level, whereas ES has the advantage that it captures this tails risk. Though, as pointed out by Yamai and Yoshiba (2005), ES

is less reliable to estimate for fat-tailed distributions, which we face in electricity markets. For a comprehensive risk monitoring, it is recommended to take into account both, VaR and ES.

The high forecasting performance of the TA-fCKDE model is reflected in the accuracy of both risk measures. It considers the risk of market price fluctuations, the effects of the interaction between demand and renewable infeed, spike risk and the time-varying behavior of the risk factors in the electricity spot market. Our methodology can as well be used to compute other risk measure, as e.g. Risk adjusted Return on Capital (RAROC), which was used by Prokopczuk et al. (2007) to quantify risks related to wholesale electricity contracts.
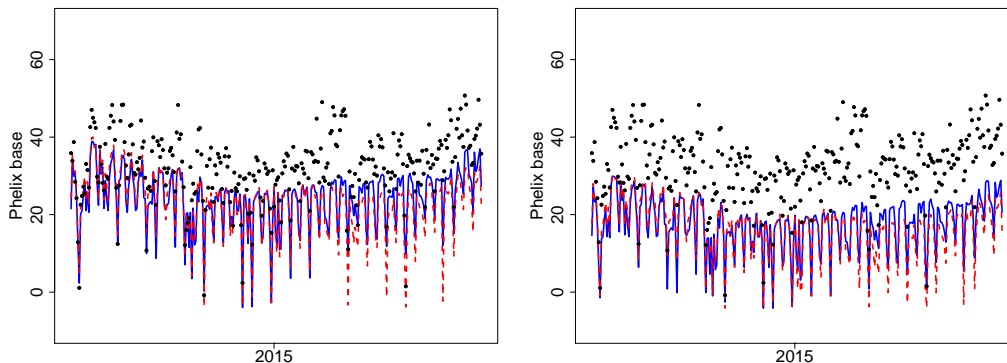
Figure 9: Observed load (black dots) together with estimated 1% VaR (left panel) and 1% expected shortfall (right panel) for TA-fCKDE (blue solid line) and fCKDE (red dashed line).

7. Conclusion

Since electricity markets have been liberalized in many countries, price forecasting is becoming an important task. Residual load - the difference between consumption and renewable infeed - plays a key role in the electricity price formation. For the purpose of modeling and forecasting electricity spot prices, a new prediction methodology that considers the uncertainty of future residual load and its stochastic relationship with prices is proposed. The methodology yields forecasts of the whole density of electricity prices, which is of great value for trading and risk management. It is able to capture spike risk associated with tail events, which is especially relevant in electricity markets. We find that the location as well as the shape of the price distribution depends on residual load. Predicted price distributions are generally asymmetric and fat-tailed. We evaluate density forecasts as well as point and interval forecasts derived from the methodology against several benchmark methods and find that the proposed methodology performs best in almost all cases. Moreover, we demonstrate how to apply the methodology to risk management and derive risk measures from the predicted densities. A possible further application would be futures pricing, as e.g. done by Bierbrauer et al. (2007).

References

Acerbi, C. and Tasche, D. (2002), "On the coherence of expected shortfall," *Journal of Banking & Finance*, 26, 1487–1503.

Aloui, C. (2008), "Value-at-risk analysis for energy commodities: long-range dependencies and fat-tails in return innovations," *Journal of Energy Markets*, 1, 31–63.

Antoch, J., Prchal, L., De Rosa, M. R., and Sarda, P. (2008), "Functional linear regression with functional response: application to prediction of electricity consumption," in *Functional and Operational Statistics*, Springer, pp. 23–29.

Artzner, P., Delbaen, F., Eber, J.-M., and Heath, D. (1999), "Coherent measures of risk," *Mathematical finance*, 9, 203–228.

Bello, A., Reneses, J., Muñoz, A., and Delgadillo, A. (2015), "Probabilistic forecasting of hourly electricity prices in the medium-term using spatial interpolation techniques," *International Journal of Forecasting*.

Bierbrauer, M., Menn, C., Rachev, S. T., and Trück, S. (2007), "Spot and derivative pricing in the EEX power market," *Journal of Banking & Finance*, 31, 3462–3485.

BMWi (2016), "Zeitreihen zur Entwicklung der erneuerbaren Energien in Deutschland," .

Bunn, D., Andresen, A., Chen, D., and Westgaard, S. (2016), "Analysis and Forecasting of Electricity Price Risks with Quantile Factor Models," *The Energy Journal*, 37(1).

Chan, K. F. and Gray, P. (2006), "Using extreme value theory to measure value-at-risk for daily electricity spot prices," *International Journal of Forecasting*, 22, 283–300.

Cuaresma, J. C., Hlouskova, J., Kossmeier, S., and Obersteiner, M. (2004), "Forecasting electricity spot-prices using linear univariate time-series models," *Applied Energy*, 77, 87–106.

Delbaen, F. (2002), "Coherent risk measures on general probability spaces," in *Advances in finance and stochastics*, Springer, pp. 1–37.

Diebold, F. X., Gunther, T. A., and Tay, A. S. (1998), "Evaluating Density Forecasts with Applications to Financial Risk Management," *International Economic Review*, 863–883.

Duffie, D. and Pan, J. (1997), "An overview of value at risk," *The Journal of derivatives*, 4, 7–49.

Eydeland, A. and Wolyniec, K. (2003), *Energy and power risk management: New developments in modeling, pricing, and hedging*, vol. 206, John Wiley & Sons.

Ferraty, F. and Vieu, P. (2006), *Nonparametric functional data analysis: theory and practice*, Springer.

Füss, R., Adams, Z., and Kaiser, D. G. (2010), "The predictive power of value-at-risk models in commodity futures markets," *Journal of Asset Management*, 11, 261–285.

Giot, P. and Laurent, S. (2003), "Market risk in commodity markets: a VaR approach," *Energy Economics*, 25, 435–457.

Gneiting, T. (2011), "Quantiles as optimal point forecasts," *International Journal of Forecasting*, 27, 197–207.

Gneiting, T. and Katzfuss, M. (2014), "Probabilistic forecasting," *Annual Review of Statistics and Its Application*, 1, 125–151.

Goia, A., May, C., and Fusai, G. (2010), "Functional clustering and linear regression for peak load forecasting," *International Journal of Forecasting*, 26, 700–711.

Hamill, T. M. (2001), "Interpretation of rank histograms for verifying ensemble forecasts," *Monthly Weather Review*, 129, 550–560.

Holton, G. A. (2003), *Value-at-risk: theory and practice*, vol. 2, Academic Press New York.

Hong, T., Pinson, P., Fan, S., Zareipour, H., Troccoli, A., and Hyndman, R. J. (2016), "Probabilistic energy forecasting: Global energy forecasting competition 2014 and beyond," *International Journal of Forecasting*, 32, 896–913.

Hörmann, S. and Kokoszka, P. (2010), "Weakly dependent functional data," *The Annals of Statistics*, 38, 1845–1884.

Horváth, L. and Kokoszka, P. (2012), *Inference for Functional Data with Applications*, Springer.

Hu, S. (2009), "Unit-price procurement auctions: structural results and comparisons," Ph.D. thesis, University of Michigan.

Jeon, J. and Taylor, J. W. (2012), "Using conditional kernel density estimation for wind power density forecasting," *Journal of the American Statistical Association*, 107, 66–79.

Jónsson, T., Pinson, P., Madsen, H., and Nielsen, H. A. (2014), "Predictive densities for day-ahead electricity prices using time-adaptive quantile regression," *Energies*, 7, 5523–5547.

Ketterer, J. C. (2014), "The impact of wind power generation on the electricity price in Germany," *Energy Economics*, 44, 270–280.

Kristiansen, T. (2012), "Forecasting Nord Pool day-ahead prices with an autoregressive model," *Energy Policy*, 49, 328–332.

López Cabrera, B. and Schulz, F. (2016), "Forecasting generalized quantiles of electricity demand: A functional data approach," *Journal of the American Statistical Association*, DOI:10.1080/01621459.2016.1219259.

Lütkepohl, H. (2005), *New introduction to multiple time series analysis*, Springer.

Misiorek, A., Trueck, S., and Weron, R. (2006), "Point and interval forecasting of spot electricity prices: Linear vs. non-linear time series models," *Studies in Nonlinear Dynamics & Econometrics*, 10.

Nadaraya, E. A. (1964), "On estimating regression," *Theory of Probability & Its Applications*, 9, 141–142.

Nicolosi, M. and Fürsch, M. (2009), "The impact of an increasing share of RES-E on the conventional power market-the example of Germany," *Zeitschrift für Energiewirtschaft*, 33, 246–254.

Nowotarski, J. and Weron, R. (2015), "Computing electricity spot price prediction intervals using quantile regression and forecast averaging," *Computational Statistics*, 30, 791–803.

Panagiotelis, A. and Smith, M. (2008), "Bayesian density forecasting of intraday electricity prices using multivariate skew t distributions," *International Journal of Forecasting*, 24, 710–727.

Prokopczuk, M., T. Rachev, S., Schindlmayr, G., and Trück, S. (2007), "Quantifying Risk in the Electricity Business: A RAROC-based Approach," *Energy Economics*, 29(5), 1033–1049.

Ramsay, J. O. and Silverman, B. W. (2005), *Functional data analysis*, Springer.

Serinaldi, F. (2011), "Distributional modeling and short-term forecasting of electricity prices by generalized additive models for location, scale and shape," *Energy Economics*, 33, 1216–1226.

Shang, H. L. (2013), "Functional time series approach for forecasting very short-term electricity demand," *Journal of Applied Statistics*, 40, 152–168.

— (2014), "A survey of functional principal component analysis," *AStA Advances in Statistical Analysis*, 98, 121–142.

Steinwart, I., Christmann, A., et al. (2011), "Estimating conditional quantiles with the help of the pinball loss," *Bernoulli*, 17, 211–225.

Vilar, J. M., Cao, R., and Aneiros, G. (2012), "Forecasting next-day electricity demand and price using nonparametric functional methods," *International Journal of Electrical Power & Energy Systems*, 39, 48–55.

Wagner, A. (2014), "Residual Demand Modeling and Application to Electricity Pricing," *The Energy journal*, 35, 45–73.

Wan, C., Xu, Z., Wang, Y., Dong, Z. Y., and Wong, K. P. (2014), "A hybrid approach for probabilistic forecasting of electricity price," *IEEE Transactions on Smart Grid*, 5, 463–470.

Watson, G. S. (1964), "Smooth regression analysis," *Sankhyā: The Indian Journal of Statistics, Series A*, 359–372.

Weron, R. (2014), "Electricity price forecasting: A review of the state-of-the-art with a look into the future," *International Journal of Forecasting*, 30, 1030–1081.

Weron, R. and Misiorek, A. (2008), "Forecasting spot electricity prices: A comparison of parametric and semiparametric time series models," *International Journal of Forecasting*, 24, 744–763.

Woo, C.-K., Horowitz, I., Moore, J., and Pacheco, A. (2011), "The impact of wind generation on the electricity spot-market price level and variance: The Texas experience," *Energy Policy*, 39, 3939–3944.

Würzburg, K., Labandeira, X., and Linares, P. (2013), "Renewable generation and electricity prices: Taking stock and new evidence for Germany and Austria," *Energy Economics*, 40, S159–S171.

Yamai, Y. and Yoshiba, T. (2005), "Value-at-risk versus expected shortfall: A practical perspective," *Journal of Banking & Finance*, 29, 997–1015.

SFB 649 Discussion Paper Series 2016

001   "Downside risk and stock returns: An empirical analysis of the long-run and short-run dynamics from the G-7 Countries" by Cathy Yi-Hsuan Chen, Thomas C. Chiang and Wolfgang Karl Härdle, January 2016.

002   "Uncertainty and Employment Dynamics in the Euro Area and the US" by Aleksei Netsunajev and Katharina Glass, January 2016.

003   "College Admissions with Entrance Exams: Centralized versus Decentralized" by Isa E. Hafalir, Rustamdjan Hakimov, Dorothea Kübler and Morimitsu Kurino, January 2016.

004   "Leveraged ETF options implied volatility paradox: a statistical study" by Wolfgang Karl Härdle, Sergey Nasekin and Zhiwu Hong, February 2016.

005   "The German Labor Market Miracle, 2003 -2015: An Assessment" by Michael C. Burda, February 2016.

006   "What Derives the Bond Portfolio Value-at-Risk: Information Roles of Macroeconomic and Financial Stress Factors" by Anthony H. Tu and Cathy Yi-Hsuan Chen, February 2016.

007   "Budget-neutral fiscal rules targeting inflation differentials" by Maren Brede, February 2016.

008   "Measuring the benefit from reducing income inequality in terms of GDP" by Simon Voigts, February 2016.

009   "Solving DSGE Portfolio Choice Models with Asymmetric Countries" by Grzegorz R. Dlugoszek, February 2016.

010   "No Role for the Hartz Reforms? Demand and Supply Factors in the German Labor Market, 1993-2014" by Michael C. Burda and Stefanie Seele, February 2016.

011   "Cognitive Load Increases Risk Aversion" by Holger Gerhardt, Guido P. Biele, Hauke R. Heekeren, and Harald Uhlig, March 2016.

012   "Neighborhood Effects in Wind Farm Performance: An Econometric Approach" by Matthias Ritter, Simone Pieralli and Martin Odening, March 2016.

013   "The importance of time-varying parameters in new Keynesian models with zero lower bound" by Julien Albertini and Hong Lan, March 2016.

014   "Aggregate Employment, Job Polarization and Inequalities: A Transatlantic Perspective" by Julien Albertini and Jean Olivier Hairault, March 2016.

015   "The Anchoring of Inflation Expectations in the Short and in the Long Run" by Dieter Nautz, Aleksei Netsunajev and Till Strohsal, March 2016.

016   "Irrational Exuberance and Herding in Financial Markets" by Christopher Boortz, March 2016.

017   "Calculating Joint Confidence Bands for Impulse Response Functions using Highest Density Regions" by Helmut Lütkepohl, Anna Staszewska-Bystrova and Peter Winker, March 2016.

018   "Factorisable Sparse Tail Event Curves with Expectiles" by Wolfgang K. Härdle, Chen Huang and Shih-Kang Chao, March 2016.

019   "International dynamics of inflation expectations" by Aleksei Netšunajev and Lars Winkelmann, May 2016.

020   "Academic Ranking Scales in Economics: Prediction and Imdputation" by Alona Zharova, Andrija Mihoci and Wolfgang Karl Härdle, May 2016.
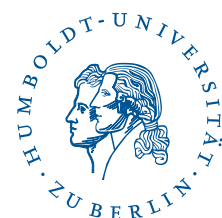
SFB 649 Discussion Paper Series 2016

For a complete list of Discussion Papers published by the SFB 649, please visit http://sfb649.wiwi.hu-berlin.de.